

---

# Discrete Dictionary-based Decomposition Layer for Structured Representation Learning

---

Taewon Park<sup>1</sup> Hyun-Chul Kim<sup>1</sup> Minho Lee<sup>1,2</sup>

<sup>1</sup>Kyungpook National University, South Korea

<sup>2</sup>ALI Co., Ltd., South Korea

ptw7998@gmail.com, hyunchul\_kim@knu.ac.kr, mholee@gmail.com

## Abstract

Neuro-symbolic neural networks have been extensively studied to integrate symbolic operations with neural networks, thereby improving systematic generalization. Specifically, Tensor Product Representation (TPR) framework enables neural networks to perform differentiable symbolic operations by encoding the symbolic structure of data within vector spaces. However, TPR-based neural networks often struggle to decompose unseen data into structured TPR representations, undermining their symbolic operations. To address this decomposition problem, we propose a **Discrete Dictionary-based Decomposition (D3)** layer designed to enhance the decomposition capabilities of TPR-based models. D3 employs discrete, learnable key-value dictionaries trained to capture symbolic features essential for decomposition operations. It leverages the prior knowledge acquired during training to generate structured TPR representations by mapping input data to pre-learned symbolic features within these dictionaries. D3 is a straightforward drop-in layer that can be seamlessly integrated into any TPR-based model without modifications. Our experimental results demonstrate that D3 significantly improves the systematic generalization of various TPR-based models while requiring fewer additional parameters. Notably, D3 outperforms baseline models on the synthetic task that demands the systematic decomposition of unseen combinatorial data.

## 1 Introduction

Compositional generalization, aiming at understanding unseen data by combining known concepts, is essential for neural networks to handle complex tasks [2, 13, 12, 15, 8, 6]. Tensor Product Representation (TPR) framework [32] facilitates this by embedding the symbolic structure of data within vector spaces, providing neural networks with compositional capabilities. Within this framework, objects are represented by a tensor product of symbolic components called *roles* and *fillers*, and these representations subsequently are superimposed to represent multiple objects in a single representation. During decoding, a specific *filler* is retrieved from the superimposed representation through matrix multiplication using an *unbinding operator* correlated to a particular *role*. This retrieved *filler* is then utilized in downstream tasks. Based on this property, TPR-based neural networks have demonstrated significant generalization and applicability in fields such as associative reasoning [27, 29], mathematical problem-solving [28], and natural language processing [9, 31, 20, 33].

Despite their successes, the TPR-based approaches pose a significant challenge known as a decomposition problem [32, 22], which refers to the difficulty of decomposing input data into TPR components, such as *roles*, *fillers*, and *unbinding operators*. Without accurate decomposition, TPR-based models fail to represent the symbolic structure of data, causing a decline in the performance of the TPR operations. Recently, inspired by an object-centric learning method [17], Park et al. [22] proposes an attention-based iterative decomposition (AID) module to address this issue. AID uses competitive

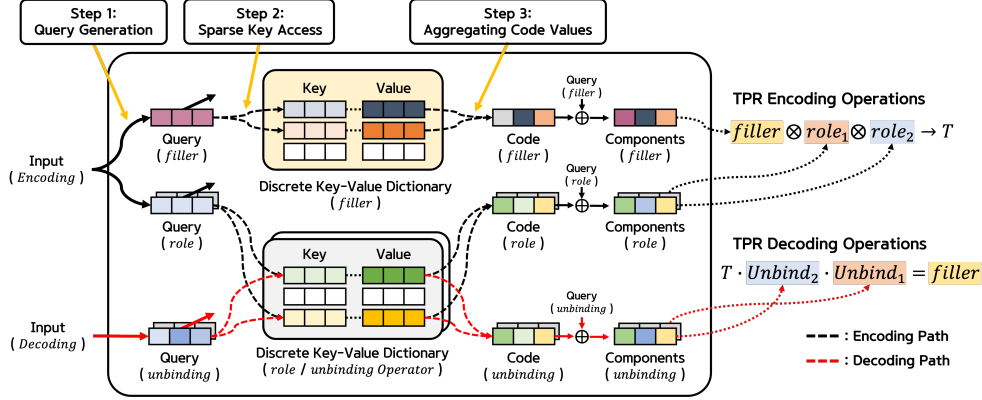


Figure 1: **Overview of D3.** D3 generates structured TPR representations by mapping input data to the nearest pre-learned symbolic features stored within discrete, learnable dictionaries. Each dictionary is linked explicitly to specific TPR components, such as *roles*, *filler*, and *unbinding operators*. Notably, D3 uses a shared dictionary configuration between the *roles* and *unbinding operators*. This figure illustrates, for example, that  $role_1$  and  $unbind_1$  share one dictionary, while  $role_2$  and  $unbind_2$  share another.  $T$  denotes a superimposed representation that represents multiple objects.

attention to iteratively refine structured representations, thereby enhancing the systematic generalization of TPR-based models. However, it still struggles to generalize all possible combinations of known symbols in simple synthetic tasks. This failure is likely attributable to its insufficient mechanism for explicitly mapping input data to known symbolic features observed during training. Therefore, the decomposition module may need an additional mechanism to store observed symbolic features during training and utilize it to effectively decompose unseen combinatorial data of known symbols.

In another line of work, discrete representation learning has been explored to improve the efficiency, interpretability, and generalization capabilities of neural networks [38, 14, 16, 36, 7]. This approach involves mapping continuous input data into discrete representations by finding the nearest features in a predefined codebook. The features within the codebook are learnable parameters, specifically trained to capture the latent features of data during training phase [38]. Some researchers have applied discrete representation techniques to extract specific types of representations from unstructured data [11, 42, 43]. Other researchers have integrated discrete symbolic embeddings within the TPR framework to improve its interpretability [20, 9]. However, these methods are designed for specific applications, such as question-answering and summarization tasks, making them difficult to integrate into other TPR-based models.

In this work, we propose a **Discrete Dictionary-based Decomposition (D3)** layer for structured representation learning within the TPR framework. D3 employs the discrete representations techniques to utilize prior knowledge acquired during training for decomposition operations. Inspired by prior discrete key-value architectures [14, 37], D3 consists of multiple dictionaries, each comprising discrete, learnable key-value pairs. Unlike prior work, each dictionary of D3 is linked explicitly to individual TPR components, such as *role*, *filler*, and *unbinding operator*. This design allows each dictionary to capture and store the symbolic features of its corresponding TPR components during training. D3 acts as a drop-in layer that maps input data into pre-learned symbolic features for the decomposition of TPR components through a three-step process, as illustrated in Fig. 1. First, it generates multiple queries from the input data, with each query utilized for different TPR components. Next, it identifies the nearest codebook keys within each dictionary based on these queries. Finally, D3 generates structured TPR representations by aggregating the codebook values corresponding to these keys. Moreover, D3 can be seamlessly integrated into any TPR-based model by replacing the TPR component generation layer without requiring further modifications.

**Our main contributions** are as follows.

- We propose a novel D3 layer to tackle the decomposition problem inherent in the TPR-based approaches. D3 leverages discrete, learnable dictionaries to enhance the decomposition capabilities of TPR-based models. By mapping input data to pre-learned symbolic features stored within the dictionaries, D3 effectively generates structured TPR representations.

- We conduct extensive experiments across various systematic generalization tasks, including synthetic associative recall and text/visual question-answering tasks. Our experimental results show that D3 significantly enhances the generalization performance of TPR-based models, demonstrating its effectiveness on systematic generalization tasks.
- Our analyses show that D3 generates well-bound structured representations that are satisfactory for the requirements of the TPR framework, utilizing the discrete, learnable dictionaries.

## 2 Related Work

**Decomposition Problem.** Compositional generalization in neural networks, which allows for generalizing beyond training data, has been extensively studied [2, 13, 12, 15, 8, 6, 40]. One important capability for achieving this is a *segregation*, as discussed in Greff et al. [6], which enables the formation of meaningful representations from structured and unstructured data [3, 17]. TPR-based neural networks also rely on this capability to generate structured representations for TPR components such as *roles*, *fillers*, and *unbinding operators*. In the TPR framework, these structured representations must satisfy specific conditions to ensure accurate encoding and decoding. First, *roles* need to be linearly independent to avoid *filler* overlap. Second, the *unbinding operator* must correlate with the corresponding *roles* to accurately retrieve associated *fillers*. Recent work [22] has shown that existing TPR-based models often fail to generate structured representations that meet these conditions, undermining their symbolic operations. To address this, an attention-based decomposition module [22] has been introduced, but it still shows limited performance on synthetic tasks involving the decomposition of unseen combinatorial data. In this work, we address the decomposition problem within the TPR framework using a discrete dictionary-based method, advancing the research further.

**Discrete Representation Learning.** Discrete neural representation learning has introduced a codebook of discrete, learnable representations into neural networks [38]. During training, each discrete representation captures underlying latent features by mapping continuous input data to the nearest features within the codebook, which are then used for downstream tasks. Recent work on object-centric learning has utilized discrete representations to extract specific types of features from unstructured data, leveraging latent features learned during training [11, 42]. Some researchers have proposed a separate key-value codebook for learning discrete representations, demonstrating its effectiveness in systematic generalization [16] and robustness against distributional shifts [37]. Inspired by these findings, we develop a separate key-value-based discrete dictionary method to enhance the decomposition capabilities of TPR-based models. Other researchers have introduced a discrete symbolic embedding layer to improve the interpretability of TPR-based models, showing the feasibility of discrete representations in the TPR framework [20, 9]. However, their methods focus on encoding processes and specific tasks such as question-answering [20] and abstractive summarization [9]. In contrast, our work addresses the decomposition problem in TPR-based approaches, and our D3 method is a drop-in solution that can be easily adapted to any TPR-based model.

**Memory Network.** Research on memory networks has focused on enhancing neural network capacity by integrating external memory [35, 4, 5, 23, 26, 40]. Memory-augmented neural networks store variable lengths of sequential data in this external memory and retrieve necessary information using various addressing methods [35, 5]. These writing and reading mechanisms share many similarities with our D3 approach. However, while memory networks store input features sequentially in their memory states as a continuous stream, D3 updates symbolic feature information through gradient descent into codebook parameters within dictionaries. This distinctive characteristic allows D3 to leverage the learned symbolic features to decompose unseen data after training. In another work, Lample et al. [14] introduces a learnable key-value memory layer to improve the efficiency of the Transformer by replacing the feed-forward layer. Unlike their memory layer, D3 employs key-value pairs in dictionaries explicitly linked to individual TPR components, making it well-suited for the TPR framework.

## 3 Method

In this section, we explain how the D3 module generates structured representations of the TPR components using discrete, learnable dictionaries. We then introduce configurations of D3 and how it can be applied to our baseline models.

### 3.1 Discrete Dictionary-based Decomposition module

D3 is a discrete dictionary-based drop-in layer designed to enhance the decomposition capabilities of TPR-based approaches. At every time step, D3 decomposes input data into TPR components, such as *roles*, *fillers*, and *unbinding operators*, by mapping input data to pre-learned symbolic features within dictionaries. These dictionaries consist of discrete, learnable codebook key-value pairs, denoted as  $\{\mathcal{D}^j\}_{j=1}^{N_{\text{component}}}$  as shown in Eq. 1. Each dictionary  $\mathcal{D}^j$  is explicitly linked to a  $j$ -th TPR component, allowing it to learn the symbolic features required for generating the specific TPR component. This design also enables the generation of structured representations for different TPR components individually and in parallel.

$$\mathcal{D}^j := \{(\mathbf{k}_i^j, \mathbf{v}_i^j) \mid \mathbf{k}_i^j \in \mathbb{R}^{D_{\text{query}}}, \mathbf{v}_i^j \in \mathbb{R}^{D_{\text{code}}}\}_{i=1}^{N_{\text{code}}} \quad \text{where } j = 1, \dots, N_{\text{component}} \quad (1)$$

where  $\mathcal{D}^j$  denotes the discrete, learnable dictionary for the  $j$ -th TPR component,  $\mathbf{k}$  denotes a learnable codebook key, and  $\mathbf{v}$  denotes a learnable codebook value. In the next paragraph, we describe how D3 generates TPR components using these dictionaries in three steps.

**Step 1: Query Generation.** At each time step  $t$ , D3 takes input data, denoted as  $\text{input}_t \in \mathbb{R}^{D_{\text{input}}}$ , and generates the query, denoted as  $\text{queries}_t \in \mathbb{R}^{N_{\text{component}} \times D_{\text{input}}}$ , for each  $j$ -th TPR component using a query network,  $f_{\text{query}}^j : \text{input}_t \mapsto \text{query}_t^j \in \mathbb{R}^{D_{\text{query}}}$ . The query network can be any neural network; in this study, we use a feed-forward network with a single layer. Additionally, we apply a layer normalization [1] and a dropout of  $p_{\text{dropout}}$  [34] to  $\text{query}_t^j$ .

**Step 2: Sparse Key Access.** D3 searches for the nearest keys from each dictionary,  $\mathcal{D}^j$ , based on the generated query  $\text{query}_t^j$ . We measure the similarity using the inner product between  $\text{query}_t^j$  and  $\{\mathbf{k}_i^j\}_{i=1}^{N_{\text{code}}}$ . Then, D3 selects top- $k$  codebook keys in order of largest similarity, as follows.

$$\mathcal{I}^j = \mathcal{T}_k(\text{query}_t^j \top \hat{\mathbf{K}}_i^j) \quad \text{where } \hat{\mathbf{K}}_i^j = \mathbf{k}_i^j / \|\mathbf{k}_i^j\|_2 \quad (2)$$

where  $\mathcal{T}_k$  denotes the top- $k$  operator that finds the indices of  $k$  largest values, and  $\mathcal{I}^j$  denotes the indices of the  $k$  most similar keys within  $\mathcal{D}^j$ . We found that applying  $L2$  normalization to keys before the inner product mitigates the codebook collapse problem.

**Step 3: Aggregation of Code Values.** D3 computes the normalized score for selected codebook keys, denoted as  $w_t^j$ , and aggregates codebook values corresponding to selected codebook keys with  $w_t^j$ , as follows.

$$\text{code}_t^j = \sum_{i \in \mathcal{I}} w_{t,i}^j \mathbf{v}_i^j \quad \text{where } w_t^j = \text{Softmax}(\text{query}_t^j \top \hat{\mathbf{K}}_i^j)_{i \in \mathcal{I}} \quad (3)$$

Then, D3 maps  $\text{query}_t^j$  to a dimension of  $D_{\text{code}}$  and adds this projected vector to  $\text{code}_t^j$ . The summed vectors are mapped to a dimension of  $D_{\text{component}}$  to generate structured representations of TPR components, as follows.

$$\text{component}_t^j = \text{code}_t^j + \text{layer}_{\text{residual}}(\text{query}_t^j) \in \mathbb{R}^{D_{\text{code}}} \quad (4)$$

$$\overline{\text{component}}_t^j = \text{layer}_{\text{final}}(\text{component}_t^j) \in \mathbb{R}^{D_{\text{component}}} \quad (5)$$

where  $\text{layer}_{\text{residual}}$  and  $\text{layer}_{\text{final}}$  denote a feed-forward network with a single layer. Those  $\overline{\text{components}}_t$  are then utilized for TPR operations to solve the downstream tasks.

### 3.2 Module Configurations

In this section, we describe the configurations of D3 when applied to TPR-based models.

**Shared Dictionary between Role and Unbinding Operator.** As discussed in Section 2, *roles* and *unbinding operators* should have correlated features for accurate TPR operations. Considering this characteristic of the TPR framework, we share the dictionaries of *roles* and *unbinding operators*. This shared dictionary also reduces the number of learnable parameters.

**D3 Applied to Filler.** While the TPR framework requires specific conditions for *roles* and *unbinding operators* for accurate TPR operations, there are no such requirements for *fillers*. Therefore, we explore two configurations in this study: applying D3 to generate *fillers* (*w/ F*) and not applying D3 to generate fillers (*w/o F*). In the *w/o F* configuration, we follow the baseline models to generate the *filler* representations.

### 3.3 Integration of D3 into Existing TPR-based Models

In this section, we introduce our baseline models and explain how D3 is applied to them, considering the configurations of D3. We use three TPR-based models as our baselines: FWM [29], TPR-RNN [27], and Linear Transformer [10]. Notably, integrating D3 into these baseline models requires only substituting their TPR component generation layer with D3 without further modifications.

**Fast Weight Memory.** Fast Weight Memory (FWM) [29] is a TPR-based memory network designed for understanding long sequential contexts. It proposes a single word-level TPR operation related to the perceptron learning rule [24]. It has shown significant associative reasoning capability in reinforcement learning and natural language processing tasks. FWM requires two types of *roles* (*role*<sub>1</sub> and *role*<sub>2</sub>) and one *filler* for encoding, as well as two types of *unbinding operators* (*unbind*<sub>1</sub> and *unbind*<sub>2</sub>) for decoding. When D3 is integrated into FWM, it employs three dictionaries for the shared dictionary configuration: one for the *role*<sub>1</sub> and *unbind*<sub>1</sub>, another for the *role*<sub>2</sub> and *unbind*<sub>2</sub>, and the other for *filler*, as shown in Fig. 1.

**TPR-RNN.** TPR-RNN [27] is a sentence-level TPR-based memory network designed for basic text question-answering tasks [41]. It incorporates various encoding operations such as writing, moving, and backlink to process sequential data at the sentence level. These operations necessitate different encoding components with varying dimensions, making direct connections to the decoding components challenging. As a result, we do not apply the shared dictionary configuration to TPR-RNN; instead, we use a shared query network without layer normalization. Furthermore, due to the differing dimensions of the TPR components in TPR-RNN, we employ distinct layer<sub>final</sub> layers for each TPR component.

**Linear Transformer.** Linear Transformer [10] linearizes the attention mechanism to improve the computational efficiency of the Transformer [39]. Recently, Schlag et al. [30] demonstrated the equivalence between TPR and the linear attention mechanism, indicating that the key, value, and query in linear attention correspond to the *role*, *filler*, and *unbinding operator*, respectively. Building on this work, we apply D3 to generate the query, key, and value in the Linear Transformer. Unlike TPR-RNN and FWM, the Linear Transformer utilizes multi-head operations. Therefore, we use distinct dictionaries for each head, with the key and query of each head sharing the same dictionary.

## 4 Experiment

In this section, we evaluate the effectiveness of D3 across various tasks, including a synthetic task, text/visual question-answering tasks, and a language modeling task. To assess the decomposition capabilities, we follow the experimental settings of the AID [22], a prior work addressing the decomposition problem in the TPR framework, and closely compare our D3 model to baseline models and AID.

### 4.1 Task

**Systematic Associative Recall (SAR) task.** This task evaluates systematic generalization in memorizing and recalling combinatorial data [22]. It consists of a discovery phase and an inference phase. During the discovery phase, the model receives the combinatorial sequential items, each combining two symbols,  $x \in X$  and  $y \in Y$  where  $X = X_1 \cup X_2$  and  $Y = Y_1 \cup Y_2$ . The model is then required to predict an associated  $y$  when a specific  $x$  is presented. The SAR task uses different combination settings between training and evaluation to target systematic generalization specifically. During training, the model learns the following combination settings: (1)  $X_1$  and  $Y_1$  and (2)  $X_2$  and  $Y_2$ . At the evaluation, on the other hand, the model should generalize unseen combination settings, specifically  $X_1$  and  $Y_2$ . In the SAR task, the TPR framework regards  $x$  as the *role* and the *unbinding*

Table 1: The mean word error rate [%] on the sys-bAbI task for 10 seeds, with  $\pm$  indicating SD.

Model	w/o sys diff ( $\downarrow$ )	w/ sys diff ( $\downarrow$ )	Gap ( $\downarrow$ )	# params ( $\downarrow$ )
TPR-RNN	0.79 $\pm$ 0.16	8.74 $\pm$ 3.74	7.95	<b>0.14 M</b>
+ AID	0.69 $\pm$ 0.08	5.61 $\pm$ 1.78	4.92	0.32 M
+ D3	<b>0.65</b> $\pm$ 0.25	<b>3.50</b> $\pm$ 2.07	<b>2.85</b>	<u>0.17 M</u>
FWM	0.79 $\pm$ 0.14	2.85 $\pm$ 1.61	2.06	<b>0.73 M</b>
+ AID	<b>0.45</b> $\pm$ 0.16	<b>1.21</b> $\pm$ 0.66	<b>0.76</b>	1.23 M
+ D3 (w/o F)	0.79 $\pm$ 0.30	2.58 $\pm$ 1.12	1.79	<u>0.75 M</u>
+ D3 (w/ F)	<u>0.75</u> $\pm$ 0.17	<u>1.96</u> $\pm$ 0.88	<u>1.21</u>	<u>0.75 M</u>

operator, and  $y$  as the filler. Therefore, TPR-based models should systematically decompose the combinatorial data into structured representations by mapping  $x$  to the role and  $y$  to the filler during the discovery phase, and mapping  $x$  to the unbinding operator during the inference phase to solve this task.

**Systematic bAbI (sys-bAbI) task.** This task is a variant of the bAbI task [41] designed to evaluate systematic generalization in text understanding and reasoning [22]. It consists of 20 distinct sub-tasks, each comprising stories, relevant queries, and corresponding answers. The sys-bAbI task requires the models to remember the stories and predict corresponding answers to the queries. Unlike the original bAbI task, the sys-bAbI task evaluates the models with two aspects: (a) in-distribution (w/o sys diff) and (b) with the systematic difference (w/ sys diff) where each sub-task includes unseen words during training. Therefore, the models should learn task-independent text understanding to solve the sys-bAbI task.

**Sort-of-CLEVR task.** This task [25] evaluates compositional generalization in visual relational reasoning. It consists of scene images, queries, and corresponding answers. This task requires the models to understand the properties of individual objects (*Unary*) or the relationships between multiple objects (*Binary* or *Ternary*) within visual scene images, and predict the correct answers to the queries [19]. Therefore, the model should capture relationships within each object and between objects to solve this task.

**WikiText-103 task.** This task [18] is a large-scale language modeling dataset consisting of lengthy corpora from Wikipedia. Although the WikiText-103 task does not directly measure the systematic generalization of the models, it is used to evaluate the effectiveness and applicability of D3 on a large-scale task beyond relatively simple tasks.

## 4.2 Experimental Results

In this section, we present the experimental results of the SAR task, sys-bAbI task, sort-of-CLEVR task, and WikiText-103 task. In our experiments, we set  $D_{\text{query}}$  as  $D_{\text{code}}/2$ .

### 4.2.1 TPR-based Memory Networks

First, we evaluate FWM with D3 on the SAR task, which requires understanding the composition of two types of symbols,  $x$  and  $y$ . TPR-based models are expected to solve this task perfectly by mapping each symbol to a specific TPR component during decomposition. However, as shown in Fig. 2, FWM and AID fail to generalize unseen combinations of known symbols. In contrast, our D3 module significantly outperforms other baseline models, achieving nearly 100% accuracy. This result demonstrates that D3 effectively decomposes unseen combinatorial data into TPR components using discrete dictionaries.

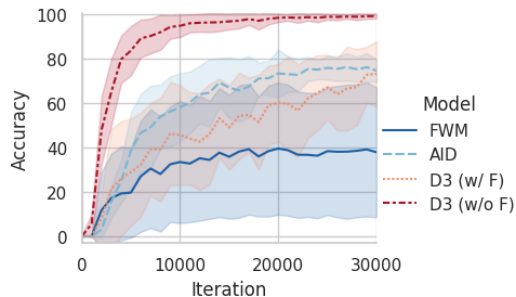


Figure 2: Test accuracy curve [%] on the SAR task for 10 seeds, with shadowed area indicating SD.

Table 2: The mean accuracy [%] on the sort-of-CLEVR task for 10 seeds, with  $\pm$  indicating SD.

Model	$D_{code}$	Unary ( $\uparrow$ )	Binary ( $\uparrow$ )	Ternary ( $\uparrow$ )	# params ( $\downarrow$ )
Linear Transformer	-	69.3 $\pm$ 14.8	75.5 $\pm$ 1.3	56.4 $\pm$ 4.3	<b>0.68 M</b>
+ AID	-	<u>98.9</u> $\pm$ 0.2	78.6 $\pm$ 0.3	63.7 $\pm$ 1.2	0.83 M
+ D3 ( <i>w/o F</i> )	128	73.9 $\pm$ 16.5	77.2 $\pm$ 2.2	57.3 $\pm$ 4.6	<u>0.75 M</u>
	256	73.7 $\pm$ 16.5	77.8 $\pm$ 2.5	57.9 $\pm$ 5.8	0.96 M
+ D3 ( <i>w/ F</i> )	128	<u>98.9</u> $\pm$ 0.2	<u>79.5</u> $\pm$ 0.8	63.1 $\pm$ 1.9	0.80 M
	256	<b>99.0</b> $\pm$ 0.3	<b>82.1</b> $\pm$ 2.4	<b>68.8</b> $\pm$ 1.2	1.13 M

Table 3: Perplexity on the WikiText-103 task.

Model	$D_{code}$	Valid ( $\downarrow$ )	Test ( $\downarrow$ )	# params ( $\downarrow$ )
Linear Transformer	-	36.473	37.533	<b>44.02 M</b>
+ AID	-	36.159	37.151	44.16 M
+ D3 ( <i>w/o F</i> )	32	<u>36.061</u>	37.220	<u>44.12 M</u>
	64	<b>35.975</b>	<b>37.009</b>	44.36 M
+ D3 ( <i>w/ F</i> )	32	36.630	37.620	44.22 M
	64	36.220	<u>37.128</u>	44.62 M

Next, we test TPR-RNN and FWM with D3 on the sys-bAbI task. This task involves compositional information in each story sentence, such as the relation between objects and their locations. It makes a sentence-level model more suitable for capturing the structural information of data than a word-level model. However, as shown in Table 1, TPR-RNN shows a larger performance gap between the *w/o sys diff* and *w/ sys diff* cases than FWM. Notably, D3 enhances the systematic generalization of both TPR-RNN and FWM with fewer additional parameters, significantly reducing the performance gap for TPR-RNN. These results highlight the efficacy of D3 in text understanding tasks.

## 4.2.2 Linear Transformer

We also evaluate the Linear Transformer with D3 on the sort-of-CLEVR task and WikiText-103 task. Following the AID [22], we use a 4-layered Linear Transformer with shared parameters for the sort-of-CLEVR task and apply D3 to a 16-layered Linear Transformer at intervals of 4 out of the 16 layers for the WikiText-103 task. As shown in Tables 2 and 3, D3 improves the performance of the Linear Transformer, with these improvements increasing as the capacity of the dictionaries grows. These results demonstrate the effectiveness of D3 on visual relational reasoning and language modeling tasks, as well as its applicability to the Linear Transformer. In addition, D3 shows comparable performance to the attention-based decomposition method, even with fewer parameters.

## 4.3 Analysis

In this section, we conduct a qualitative analysis of the structured TPR representations generated by D3 and an ablation study of D3. For these analyses, we experiment with D3 (*w/o F*) on the SAR task.

### 4.3.1 Qualitative Analysis

TPR framework requires its structured representations to satisfy the following conditions for accurate TPR operations: (i) linearly independence between distinct *roles*, and (ii) high correlation between *role* and *unbinding operator* for the same symbol  $x$ . We analyze the orthogonality of generated representations to investigate whether they satisfy these TPR conditions. Specifically, we consider the case of varying  $x$  while keeping  $y$  fixed for simplicity.

Fig. 3(c) shows the cosine similarity between the *roles* during the discovery phase, and Fig. 4(c) shows the cosine similarity between the *roles* during the discovery phase and the *unbinding operator* during the inference phase. Both results demonstrate that the generated representations by D3 satisfy the TPR conditions, resulting in an accuracy of nearly 100%. We also conduct the same analysis for intermediate features, particularly query and code. Figs. 3 and 4 show that each intermediate representation complements the others to satisfy the TPR condition, indicating the effectiveness of D3.

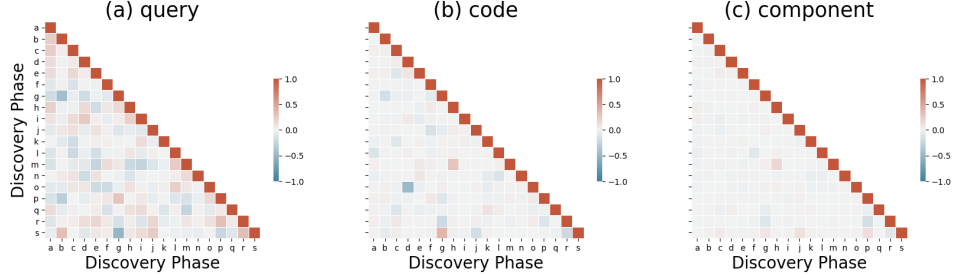


Figure 3: The heatmap displays the cosine similarity between the generated representations during the discovery phase for the SAR task. We explore the similarity across different types of representations: (a) queries of *roles*, (b) codes of *roles*, and (c) the *roles* themselves.

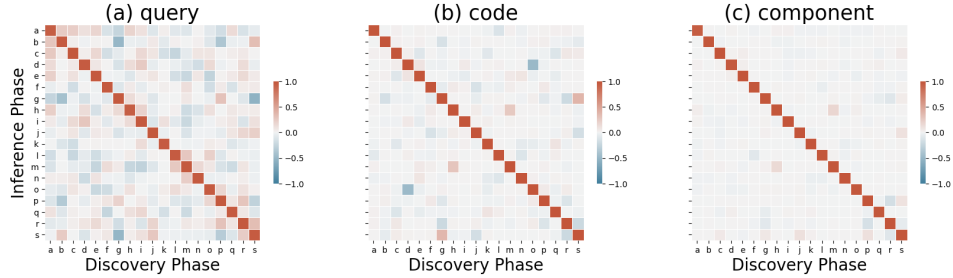


Figure 4: The heatmap displays the cosine similarity between the generated representations during the discovery phase (represented on the **x-axis**) and the inference phase (represented on the **y-axis**) for the SAR task. We explore the similarity across different types of representations: (a) queries of *roles* and *unbinding operators*, (b) codes of *roles* and *unbinding operators*, and (c) the *roles* and *unbinding operators* themselves.

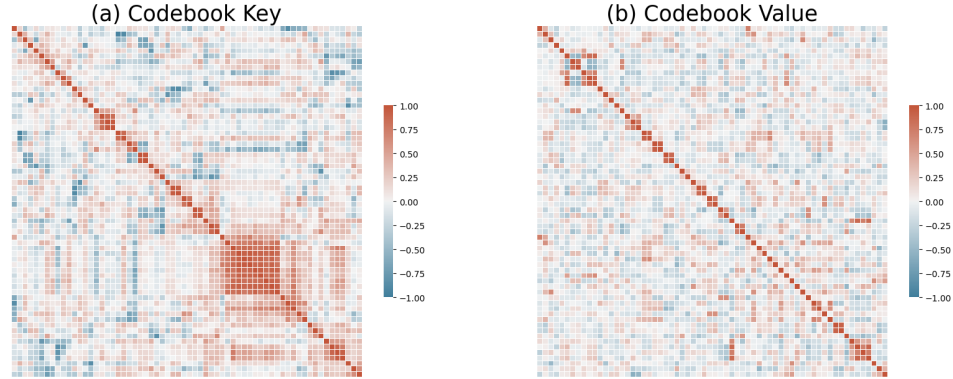


Figure 5: The heatmap visualizes the cosine similarity of the learned codebook features for the SAR task. There are two parts to each heatmap: (a) the similarity among codebook keys, denoted as  $\{\mathbf{k}_i\}_{i=1}^{N_{\text{code}}}$ , and (b) the similarity among codebook values, denoted as  $\{\mathbf{v}_i\}_{i=1}^{N_{\text{code}}}$ . For better visualization, the heatmap values are reordered to reflect the cluster of similar codebook keys.

Furthermore, we analyze the similarity patterns of codebook keys and codebook values. Fig. 5 shows that the codebook features learn orthogonal patterns despite being learned without constraints. This result implies that the learnable parameters of dictionaries implicitly capture TPR conditions to ensure accurate TPR operations.

### 4.3.2 Ablation Study

We investigate the effect of hyper-parameters of D3, specifically  $N_{\text{code}}$ ,  $D_{\text{code}}$ , and top- $k$ , on performance on the SAR task. Fig. 6(a) shows the effect of  $D_{\text{code}}$ . We observe that the value of  $D_{\text{code}}$  significantly affects the performance of D3. Notably, D3 fails to solve the SAR task when  $D_{\text{code}}$  is set



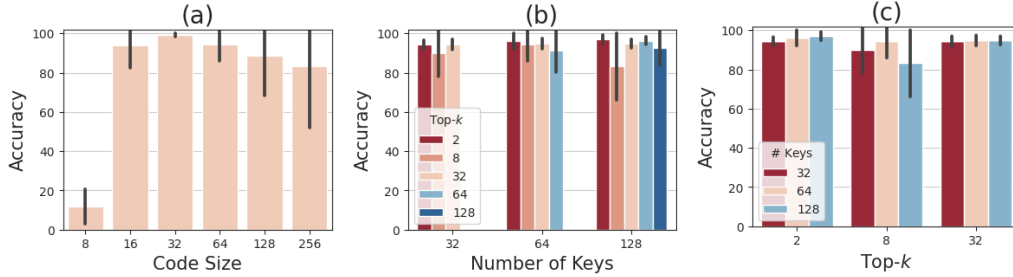


Figure 6: The mean accuracy on the SAR task for 10 seeds in the ablation study, with error bar indicating SD. The default setting uses  $D_{code}$  of 64,  $N_{code}$  of 64, and top- $k$  of 8. Each figure shows the experimental results for the following settings: (a) Varying  $D_{code}$ . (b) Varying top- $k$  with  $N_{code}$  constant. (c) Varying  $N_{code}$  with top- $k$  constant.

to 8, indicating a need for adequate capacity of  $D_{code}$ . Fig. 6(b) shows the effect of varying top- $k$  while holding  $N_{code}$  constant, indicating that D3 achieves optimal performance when top- $k$  is set to 2. This result demonstrates the efficacy of the sparse mechanism employed by D3. Fig. 6(c) examines the effect of varying  $N_{code}$  while holding top- $k$  constant, showing that D3 generally performs better with larger values of  $N_{code}$ .

## 5 Discussion and Limitations

**D3 Applied to Filler (w/o F and w/ F).** In the TPR framework, *roles* and *unbinding operators* must meet specific conditions, such as linear independence among *roles* and high correlation between *roles* and *unbinding operators*, to ensure accurate TPR operations. However, there are no such requirements for *fillers*, which are features related to downstream tasks. This characteristic affects the performance of D3 depending on whether it is applied to generate the *fillers* (w/ F) or not (w/o F). In our experiments, the w/ F configuration performs well on the sys-bAbI and sort-of-CLEVR tasks with relatively few labels (~200). In contrast, the w/o F configuration excels on the SAR and WikiText-103 tasks, which have a larger number of labels (500~). These findings suggest that the w/o F configuration may be more effective for large-scale practical tasks. Nevertheless, beyond these experimental results, we do not fully understand the conditions under which each configuration performs better. Consequently, one limitation of D3 is the additional burden of determining the suitable configuration for various tasks when applying it to other domains.

**Sparse Key Selection.** D3 integrates seamlessly with existing TPR-based models, significantly enhancing their generalization performance across various tasks. However, this integration introduces additional computational overhead to the baseline models. Specifically, the sparse key selection mechanism of D3 has a computational complexity of  $\mathcal{O}(N_{code} \times (D_{query} + \log k))$  for each TPR component. Therefore, this complexity can become a drawback as the capacity of the dictionaries increases. One potential solution to address this capacity issue is to incorporate product keys into the sparse key selection mechanism of D3, a technique studied in prior discrete key-value architectures [14]. We leave this enhancement for future work.

## 6 Conclusion

In this paper, we tackle the decomposition problem inherent in the TPR framework, which poses a significant challenge for TPR-based models. To address this, we introduce a discrete dictionary-based layer, D3, designed to enhance the decomposition capabilities of TPR-based models. D3 employs the discrete dictionaries to map input data to pre-learned symbolic features within each dictionary, thereby generating structured TPR representations. Our comprehensive experiments demonstrate that D3 significantly enhances the systematic generalization of the TPR-based models with fewer additional parameters. Furthermore, our qualitative analysis verifies that D3 effectively generates structured representations that are satisfactory for the requirements of the TPR framework.

## Acknowledgements

This work was supported by the National Research Foundation of Korea(NRF) grant funded by the Korea government(MSIT)(No. 2021R1A2C3011169) and the National Research Foundation of Korea(NRF) grant funded by the Korea government(MSIT)(No. 2022R1A5A7026673).

## References

- [1] J. L. Ba, J. R. Kiros, and G. E. Hinton. Layer normalization. *arXiv preprint arXiv:1607.06450*, 2016.
- [2] J. A. Fodor and Z. W. Pylyshyn. Connectionism and cognitive architecture: A critical analysis. *Cognition*, 28(1-2):3–71, 1988.
- [3] A. Goyal, A. Lamb, J. Hoffmann, S. Sodhani, S. Levine, Y. Bengio, and B. Schölkopf. Recurrent independent mechanisms. *arXiv preprint arXiv:1909.10893*, 2019.
- [4] A. Graves, G. Wayne, and I. Danihelka. Neural Turing machines. *arXiv preprint arXiv:1410.5401*, 2014.
- [5] A. Graves, G. Wayne, M. Reynolds, T. Harley, I. Danihelka, A. Grabska-Barwińska, S. G. Colmenarejo, E. Grefenstette, T. Ramalho, J. Agapiou, et al. Hybrid computing using a neural network with dynamic external memory. *Nature*, 538(7626):471–476, 2016.
- [6] K. Greff, S. Van Steenkiste, and J. Schmidhuber. On the binding problem in artificial neural networks. *arXiv preprint arXiv:2012.05208*, 2020.
- [7] K. Hsu, W. Dorrell, J. Whittington, J. Wu, and C. Finn. Disentanglement via latent quantization. *Advances in Neural Information Processing Systems*, 36, 2024.
- [8] D. Hupkes, V. Dankers, M. Mul, and E. Bruni. Compositionality decomposed: How do neural networks generalise? *Journal of Artificial Intelligence Research*, 67:757–795, 2020.
- [9] Y. Jiang, A. Celikyilmaz, P. Smolensky, P. Soulos, S. Rao, H. Palangi, R. Fernandez, C. Smith, M. Bansal, and J. Gao. Enriching transformers with structured tensor-product representations for abstractive summarization. *arXiv preprint arXiv:2106.01317*, 2021.
- [10] A. Katharopoulos, A. Vyas, N. Pappas, and F. Fleuret. Transformers are rnns: Fast autoregressive transformers with linear attention. In *International conference on machine learning*, pages 5156–5165. PMLR, 2020.
- [11] A. Kori, F. Locatello, F. D. S. Ribeiro, F. Toni, and B. Glocker. Grounded object-centric learning. In *The Twelfth International Conference on Learning Representations*, 2023.
- [12] B. Lake and M. Baroni. Generalization without systematicity: On the compositional skills of sequence-to-sequence recurrent networks. In *International conference on machine learning*, pages 2873–2882. PMLR, 2018.
- [13] B. M. Lake, T. D. Ullman, J. B. Tenenbaum, and S. J. Gershman. Building machines that learn and think like people. *Behavioral and brain sciences*, 40:e253, 2017.
- [14] G. Lample, A. Sablayrolles, M. Ranzato, L. Denoyer, and H. Jégou. Large memory layers with product keys. *Advances in Neural Information Processing Systems*, 32, 2019.
- [15] A. Liška, G. Kruszewski, and M. Baroni. Memorize or generalize? searching for a compositional rnn in a haystack. *arXiv preprint arXiv:1802.06467*, 2018.
- [16] D. Liu, A. M. Lamb, K. Kawaguchi, A. G. ALIAS PARTH GOYAL, C. Sun, M. C. Mozer, and Y. Bengio. Discrete-valued neural communication. *Advances in Neural Information Processing Systems*, 34:2109–2121, 2021.
- [17] F. Locatello, D. Weissenborn, T. Unterthiner, A. Mahendran, G. Heigold, J. Uszkoreit, A. Dosovitskiy, and T. Kipf. Object-centric learning with slot attention. *Advances in Neural Information Processing Systems*, 33:11525–11538, 2020.

- [18] S. Merity, C. Xiong, J. Bradbury, and R. Socher. Pointer sentinel mixture models. *arXiv preprint arXiv:1609.07843*, 2016.
- [19] S. Mittal, S. C. Rappaport, I. Rish, Y. Bengio, and G. Lajoie. Compositional attention: Disentangling search and retrieval. *arXiv preprint arXiv:2110.09419*, 2021.
- [20] H. Palangi, P. Smolensky, X. He, and L. Deng. Question-answering with grammatically-interpretable representations. In *Proceedings of the AAAI Conference on Artificial Intelligence*, volume 32, 2018.
- [21] T. Park, I. Choi, and M. Lee. Distributed associative memory network with memory refreshing loss. *Neural Networks*, 144:33–48, 2021.
- [22] T. Park, I. Choi, and M. Lee. Attention-based iterative decomposition for tensor product representation. In *The Twelfth International Conference on Learning Representations*, 2023.
- [23] J. Rae, J. J. Hunt, I. Danihelka, T. Harley, A. W. Senior, G. Wayne, A. Graves, and T. Lillicrap. Scaling memory-augmented neural networks with sparse reads and writes. In *Advances in Neural Information Processing Systems*, pages 3621–3629, 2016.
- [24] F. Rosenblatt. The perceptron: a probabilistic model for information storage and organization in the brain. *Psychological review*, 65(6):386, 1958.
- [25] A. Santoro, D. Raposo, D. G. Barrett, M. Malinowski, R. Pascanu, P. Battaglia, and T. Lillicrap. A simple neural network module for relational reasoning. *Advances in neural information processing systems*, 30, 2017.
- [26] A. Santoro, R. Faulkner, D. Raposo, J. Rae, M. Chrzanowski, T. Weber, D. Wierstra, O. Vinyals, R. Pascanu, and T. Lillicrap. Relational recurrent neural networks. *Advances in neural information processing systems*, 31, 2018.
- [27] I. Schlag and J. Schmidhuber. Learning to reason with third order tensor products. *Advances in neural information processing systems*, 31, 2018.
- [28] I. Schlag, P. Smolensky, R. Fernandez, N. Jovic, J. Schmidhuber, and J. Gao. Enhancing the transformer with explicit relational encoding for math problem solving. *arXiv preprint arXiv:1910.06611*, 2019.
- [29] I. Schlag, T. Munkhdalai, and J. Schmidhuber. Learning associative inference using fast weight memory. *arXiv preprint arXiv:2011.07831*, 2020.
- [30] I. Schlag, K. Irie, and J. Schmidhuber. Linear transformers are secretly fast weight programmers. In *International Conference on Machine Learning*, pages 9355–9366. PMLR, 2021.
- [31] Z. Shi, Q. Zhang, and A. Lipani. Steppgame: A new benchmark for robust multi-hop spatial reasoning in texts. In *Proceedings of the AAAI conference on artificial intelligence*, volume 36, pages 11321–11329, 2022.
- [32] P. Smolensky. Tensor product variable binding and the representation of symbolic structures in connectionist systems. *Artificial intelligence*, 46(1-2):159–216, 1990.
- [33] P. Soulos, E. J. Hu, K. McCurdy, Y. Chen, R. Fernandez, P. Smolensky, and J. Gao. Differentiable tree operations promote compositional generalization. In *International Conference on Machine Learning*, pages 32499–32520. PMLR, 2023.
- [34] N. Srivastava, G. Hinton, A. Krizhevsky, I. Sutskever, and R. Salakhutdinov. Dropout: a simple way to prevent neural networks from overfitting. *The journal of machine learning research*, 15(1):1929–1958, 2014.
- [35] S. Sukhbaatar, J. Weston, R. Fergus, et al. End-to-end memory networks. In *Advances in neural information processing systems*, pages 2440–2448, 2015.
- [36] A. Tamkin, M. Tauffeeque, and N. D. Goodman. Codebook features: Sparse and discrete interpretability for neural networks. *arXiv preprint arXiv:2310.17230*, 2023.

- [37] F. Träuble, A. Goyal, N. Rahaman, M. C. Mozer, K. Kawaguchi, Y. Bengio, and B. Schölkopf. Discrete key-value bottleneck. In *International Conference on Machine Learning*, pages 34431–34455. PMLR, 2023.
- [38] A. Van Den Oord, O. Vinyals, et al. Neural discrete representation learning. *Advances in neural information processing systems*, 30, 2017.
- [39] A. Vaswani, N. Shazeer, N. Parmar, J. Uszkoreit, L. Jones, A. N. Gomez, Ł. Kaiser, and I. Polosukhin. Attention is all you need. *Advances in neural information processing systems*, 30, 2017.
- [40] T. W. Webb, I. Sinha, and J. D. Cohen. Emergent symbols through binding in external memory. *arXiv preprint arXiv:2012.14601*, 2020.
- [41] J. Weston, A. Bordes, S. Chopra, A. M. Rush, B. Van Merriënboer, A. Joulin, and T. Mikolov. Towards ai-complete question answering: A set of prerequisite toy tasks. *arXiv preprint arXiv:1502.05698*, 2015.
- [42] Y.-F. Wu, M. Lee, and S. Ahn. Structured world modeling via semantic vector quantization. *arXiv preprint arXiv:2402.01203*, 2024.
- [43] X. Zhuang, Q. Zhang, K. Ding, Y. Bian, X. Wang, J. Lv, H. Chen, and H. Chen. Learning invariant molecular representation in latent discrete space. *Advances in Neural Information Processing Systems*, 36, 2024.

# Appendix

## A Experiment Details

This section provides a detailed description of our experiments on the SAR task, sys-bAbI task, sort-of-CLEVR task, and WikiText-103 task. We followed the experimental settings outlined by AID [22] to assess the decomposition capabilities of D3. To ensure stability and reproducibility, we ran all experiments, except for the WikiText-103 task, using 10 different random seeds<sup>1</sup>. For the WikiText-103 task, we experimented with a single seed of 1111. Each experiment was conducted on a single 48GB NVIDIA RTX A6000 GPU and an AMD EPYC 7513 32-Core Processor.

### A.1 Systematic Associative Recall task

The SAR task [22] evaluates systematic generalization in memorizing and recalling combinatorial data. It consists of a discovery phase and an inference phase. During the discovery phase, the model receives the combinatorial sequential items, each combining two symbols,  $x \in X$  and  $y \in Y$  where  $X = X_1 \cup X_2 \cup X_3$  and  $Y = Y_1 \cup Y_2$ . The model is then required to predict an associated  $y$  when a specific  $x$  is presented. The SAR task uses different combination settings between training and evaluation to target systematic generalization specifically. During the training, the model learns the following combination settings: (1)  $X_1$  and  $Y_1$ , (2)  $X_2$  and  $Y_2$ , and (3)  $X_3$  and  $Y$ . At evaluation, however, the model should generalize unseen combination settings, specifically  $X_1$  and  $Y_2$ . In our study, unlike the AID paper [22], we only consider the most challenging setting of the SAR task by excluding the subset  $X_3$ .

Each combinatorial item is constructed as follows. First, symbols  $x$  and  $y$  are sampled from their respective sets  $X$  and  $Y$ , where  $|X_1| = |X_2| = |Y_1| = |Y_2| = 250$ . The sampled symbols are mapped into a 50-dimensional space using a word embedding method. These embedding vectors are then concatenated to construct the combinatorial item. For training, 100 randomly generated combinatorial items are sequentially provided to the model during the discovery phase. During the inference phase, the model receives only the  $x$  symbols sequentially, with the embedding vector of  $y$  set to zero. This task also provides binary flags to indicate the start of each phase. At evaluation, all possible combinations that can be formed in  $X_1$  and  $Y_2$  are tested.

To build the experimental environment for the SAR task, we utilize the open-source implementation<sup>2</sup> from the AID [22]. We train the model using the Adam optimizer with a batch size of 64 and a learning rate of  $1e^{-3}$ ,  $\beta_1$  of 0.9, and  $\beta_2$  of 0.98 for training iterations of  $30K$ . Each experiment took approximately 3 hours per each seed.

### A.2 Systematic bAbI task

The sys-bAbI task [22] is a variant of the bAbI task [41] designed to evaluate systematic generalization in text understanding and reasoning. It consists of 20 distinct sub-tasks, each comprising stories, relevant queries, and corresponding answers. The sys-bAbI task requires the models to remember the stories and predict corresponding answers to the queries. Unlike the original bAbI task, the sys-bAbI task evaluates the models with two aspects: (a) in-distribution (*w/o sys diff*) and (b) with the systematic difference (*w/ sys diff*) where each sub-task includes unseen words during training. Therefore, the models should learn task-independent text understanding to solve the sys-bAbI task.

The bAbI dataset includes various versions, such as `en-10k` and `en-valid-10k`. The sys-bAbI task uses the `en-valid-10k` version, which is already divided into training, validation, and test datasets. To create the experimental environment for the sys-bAbI task, we use the open-source implementation<sup>3</sup> provided by the AID.

---

<sup>1</sup>We used the following seed values: {0, 1111, 2222, 3333, 4444, 5555, 6666, 7777, 8888, 9999}

<sup>2</sup><https://github.com/taewonpark/AID/tree/main/SARtask>

<sup>3</sup><https://github.com/taewonpark/AID/tree/main/bAbItask>

We use the open-source implementation of the baseline models, TPR-RNN<sup>4</sup> [27] and FWM<sup>5</sup> [29]. Following the experimental settings of baseline models, we use different configurations for each model. We train the TPR-RNN with D3 using an embedding size of 179 and the Adam optimizer with a batch size of 64 and a learning rate of  $1e^{-3}$ ,  $\beta_1$  of 0.9, and  $\beta_2$  of 0.99 for 100 training epochs. For FWM with D3, we use an embedding size of 256 and the Adam optimizer with a batch size of 64 and a learning rate of  $1e^{-3}$ ,  $\beta_1$  of 0.9, and  $\beta_2$  of 0.98 for training iterations of 60K. Furthermore, following the AID, we use the reconstruction loss for the bAbI task, introduced in Park et al. [21], in our experiments on the sys-bAbI task. Each experiment took approximately 7 hours per seed for the TPR-RNN with D3 and 8 hours per seed for the FWM with D3.

### A.3 Sort-of-CLEVR task

The sort-of-CLEVR task [25] evaluates compositional generalization in visual relational reasoning. It consists of scene images, queries, and corresponding answers. This task requires the models to understand the properties of individual objects (*Unary*) or the relationships between multiple objects (*Binary* or *Ternary*) within visual scene images and predict the correct answers to the queries. Therefore, the model should capture relationships within each object and between objects to solve this task.

Each scene image, with a size of  $75 \times 75$  pixels, includes 6 distinct objects in 6 different colors (red, blue, green, orange, yellow, or gray) and 2 different shapes (square or circle). This scene image is encoded by a visual encoder. The encoded visual feature is then concatenated with the embedding vector of the query. These concatenated features are provided to the model. Following the experimental settings of the AID [22], we use a single CNN layer with a kernel size of 15 and a stride of 15 for the visual encoder, and an embedding size of 128 for the word embedding method. Also, we use a 4-layered Transformer, where each layer shares its parameters with others, as our baseline model.

To build the experimental environment for the sort of CLEVR task, we utilize the open-source implementation<sup>6</sup> from Mittal et al. [19]. We train the model using the Adam optimizer with a batch size of 64 and a learning rate of  $1e^{-4}$  for 100 training epochs. Each experiment took approximately 2.5 hours per each seed.

### A.4 WikiText-103 task

The WikiText-103 task [18] is a large-scale language modeling dataset consisting of lengthy corpora from Wikipedia. Although the WikiText-103 task does not directly measure the systematic generalization of the models, it is used to evaluate the effectiveness and applicability of D3 on a large-scale task beyond relatively simple tasks.

The WikiText-103 task comprises 28,475 articles for training, 60 for validation, and 60 for testing. Following the experimental settings of Schlag et al. [30], we partition the articles into segments of  $L$  words. During training, the gradient is back-propagated only within spans of  $L$  words. The performance of the model is evaluated using the measure of perplexity. During evaluation, the model processes an input sequence of  $L$  words by sliding a segment over the article with a stride size of 1. Perplexity is then computed based on the last position of each segment, except for the first segment, where every position is taken into account.

To build the experimental environment for the WikiText-103 task, we utilize the open-source implementation<sup>7</sup> from [30]. Following the AID [22], we apply D3 to a 16-layered Linear Transformer at intervals of 4 out of the 16 layers. We train the model using the Adam optimizer with a batch size of 96, an initial learning rate of  $2.5e^{-4}$ , and a learning rate warmup step of 2,000 for 120 epochs. Each experiment took approximately ~3 days.

---

<sup>4</sup><https://github.com/APodolskiy/TPR-RNN-Torch>

<sup>5</sup><https://github.com/ischlag/Fast-Weight-Memory-public>

<sup>6</sup><https://github.com/sarthmit/Compositional-Attention/tree/main/Sort-of-CLEVR>

<sup>7</sup><https://github.com/IDSIA/lmtool-fwp>

## B Hyper-parameter Settings

Table 4: Hyper-parameter settings of the D3.

	SAR task	<i>sys-bAbI</i> task	Sort-of-CLEVR task	WikiText-103 task
$D_{\text{code}}$	8, 16, <u>32</u> , 64, 128	32, <u>64</u> , 128, 256	128, <u>256</u>	32, <u>64</u>
$N_{\text{code}}$	64			
$D_{\text{query}}$	$D_{\text{code}}/2$			
top- $k$	8			
$p_{\text{dropout}}$	0.1			

Table 5: Hyper-parameters of TPR-RNN.

	<i>sys-bAbI</i> task
$D_{\text{entity}} (D_{\text{component}})$	90
$D_{\text{relation}} (D_{\text{component}})$	20
$N_{\text{component}}^{\text{enc}}$	5
$N_{\text{component}}^{\text{dec}}$	4

Table 6: Hyper-parameters of FWM.

	SAR task	<i>sys-bAbI</i> task
$D_{\text{LSTM}}$	256	256
$D_{\text{FWM}} (D_{\text{component}})$	32	32
$N_{\text{reads}}$	1	3
$N_{\text{component}}^{\text{enc}}$	3	3
$N_{\text{component}}^{\text{dec}}$	$1+N_{\text{reads}}$	$1+N_{\text{reads}}$

Table 7: Hyper-parameters of Linear Transformer.

	Sort-of-CLEVR task	WikiText-103 task
$D_{\text{heads}} (D_{\text{component}})$	64	16
$N_{\text{heads}}$	4	8
$N_{\text{component}}^{\text{enc}}$	$2 * N_{\text{heads}}$	$2 * N_{\text{heads}}$
$N_{\text{component}}^{\text{dec}}$	$N_{\text{heads}}$	$N_{\text{heads}}$

## C Additional Experiments

Table 8: The mean word error rate [%] on additional experiments of the *sys-bAbI* task for 10 seeds.

<b>Model</b>	$D_{\text{code}}$	w/o <i>sys diff</i> ( $\downarrow$ )	w/ <i>sys diff</i> ( $\downarrow$ )	<b>Gap</b> ( $\downarrow$ )	# params ( $\downarrow$ )
TPR-RNN	-	0.79 $\pm$ 0.16	8.74 $\pm$ 3.74	7.95	<u>0.14</u> <i>M</i>
+ AID	-	0.69 $\pm$ 0.08	5.61 $\pm$ 1.78	4.92	0.32 <i>M</i>
+ D3	32	1.16 $\pm$ 0.25	<b>3.44</b> $\pm$ 1.78	<b>2.28</b>	<b>0.13</b> <i>M</i>
	64	<b>0.65</b> $\pm$ 0.25	<u>3.50</u> $\pm$ 2.07	<u>2.85</u>	0.17 <i>M</i>
	128	<u>0.68</u> $\pm$ 0.14	3.94 $\pm$ 2.20	3.26	0.26 <i>M</i>
FWM	-	0.79 $\pm$ 0.14	2.85 $\pm$ 1.61	2.06	<b>0.73</b> <i>M</i>
+ AID	-	<b>0.45</b> $\pm$ 0.16	<b>1.21</b> $\pm$ 0.66	<b>0.76</b>	1.23 <i>M</i>
+ D3 (w/o <i>F</i> )	64	0.79 $\pm$ 0.30	2.58 $\pm$ 1.12	1.79	0.75 <i>M</i>
	128	0.93 $\pm$ 0.20	3.82 $\pm$ 1.21	2.89	0.82 <i>M</i>
	256	1.04 $\pm$ 0.40	3.33 $\pm$ 1.21	2.29	0.97 <i>M</i>
+ D3 (w/ <i>F</i> )	32	1.20 $\pm$ 0.31	7.23 $\pm$ 4.33	6.03	<u>0.71</u> <i>M</i>
	64	<u>0.75</u> $\pm$ 0.17	<u>1.96</u> $\pm$ 0.88	<u>1.21</u>	0.75 <i>M</i>
	128	0.89 $\pm$ 0.32	2.48 $\pm$ 0.67	1.59	0.84 <i>M</i>
	256	<u>0.75</u> $\pm$ 0.23	3.09 $\pm$ 1.83	2.34	1.02 <i>M</i>



## D Additional Qualitative Analysis

Additionally, we present the results of the qualitative analysis for different seeds in the SAR task.

### D.1 $N_{\text{code}}: 64, D_{\text{code}}: 32, \text{top-}k: 8, \text{seed}: 3333$

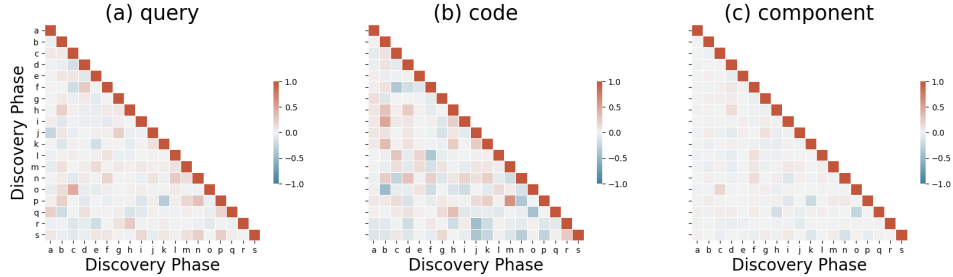


Figure 7: The heatmap displays the cosine similarity between the generated representations during the discovery phase for the SAR task. We explore the similarity across different types of representations: (a) queries of *roles*, (b) codes of *roles*, and (c) the *roles* themselves.

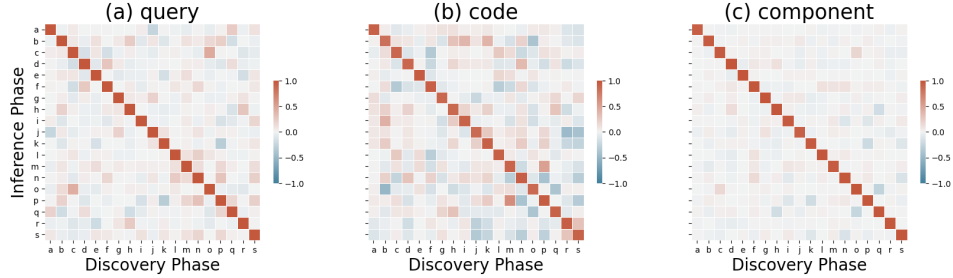


Figure 8: The heatmap displays the cosine similarity between the generated representations during the discovery phase (represented on the **x-axis**) and the inference phase (represented on the **y-axis**) for the SAR task. We explore the similarity across different types of representations: (a) queries of *roles* and *unbinding operators*, (b) codes of *roles* and *unbinding operators*, and (c) the *roles* and *unbinding operators* themselves.

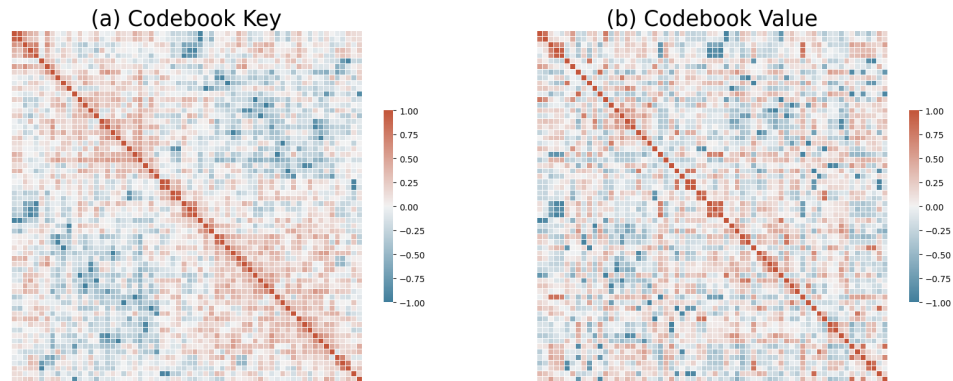


Figure 9: The heatmap visualizes the cosine similarity of the learned codebook features for the SAR task. There are two parts to each heatmap: (a) the similarity among codebook keys, denoted as  $\{k_i\}_{i=1}^{N_{\text{code}}}$ , and (b) the similarity among codebook values, denoted as  $\{v_i\}_{i=1}^{N_{\text{code}}}$ . For better visualization, the heatmap values are reordered to reflect the cluster of similar codebook keys.

D.2  $N_{\text{code}}: 64, D_{\text{code}}: 32, \text{top-}k: 8, \text{seed}: 4444$

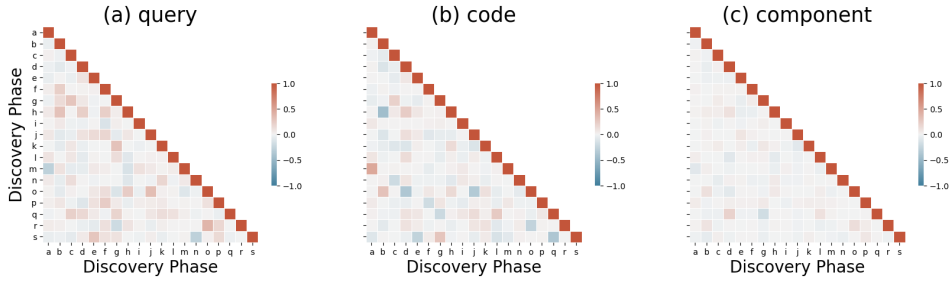


Figure 10: The heatmap displays the cosine similarity between the generated representations during the discovery phase for the SAR task. We explore the similarity across different types of representations: (a) queries of *roles*, (b) codes of *roles*, and (c) the *roles* themselves.

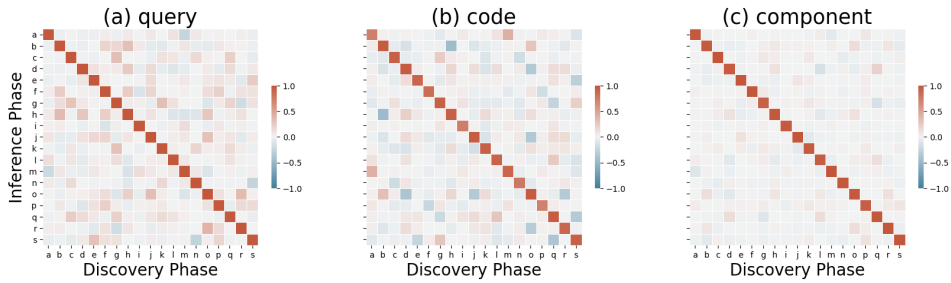


Figure 11: The heatmap displays the cosine similarity between the generated representations during the discovery phase (represented on the **x-axis**) and the inference phase (represented on the **y-axis**) for the SAR task. We explore the similarity across different types of representations: (a) queries of *roles* and *unbinding operators*, (b) codes of *roles* and *unbinding operators*, and (c) the *roles* and *unbinding operators* themselves.

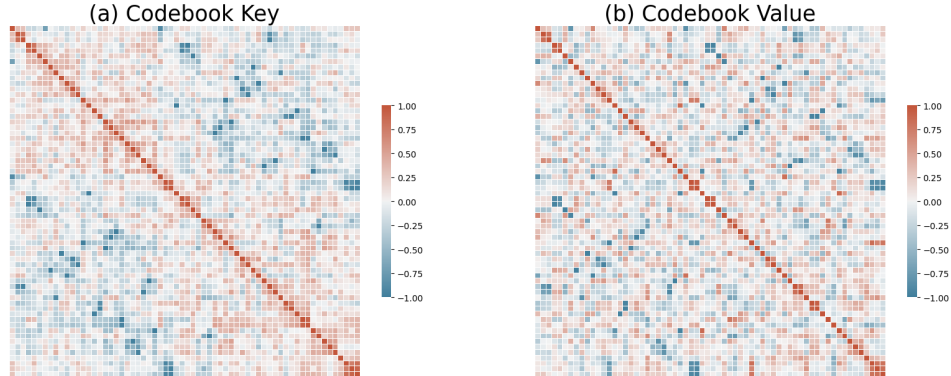


Figure 12: The heatmap visualizes the cosine similarity of the learned codebook features for the SAR task. There are two parts to each heatmap: (a) the similarity among codebook keys, denoted as  $\{k_i\}_{i=1}^{N_{\text{code}}}$ , and (b) the similarity among codebook values, denoted as  $\{v_i\}_{i=1}^{N_{\text{code}}}$ . For better visualization, the heatmap values are reordered to reflect the cluster of similar codebook keys.